

See discussions, stats, and author profiles for this publication at: <https://www.researchgate.net/publication/282360823>

# Bright-Yellow-Emissive N-Doped Carbon Dots: Preparation, Cellular Imaging, and Bifunctional Sensing

ARTICLE in ACS APPLIED MATERIALS & INTERFACES · OCTOBER 2015

Impact Factor: 6.72 · DOI: 10.1021/acsaami.5b07255

---

READS

62

## 6 AUTHORS, INCLUDING:



Jiang Kai

Chongqing University

5 PUBLICATIONS 20 CITATIONS

[SEE PROFILE](#)



Ling Zhang

Chinese Academy of Sciences

27 PUBLICATIONS 586 CITATIONS

[SEE PROFILE](#)



Congzhong Cai

Chongqing University

11 PUBLICATIONS 46 CITATIONS

[SEE PROFILE](#)

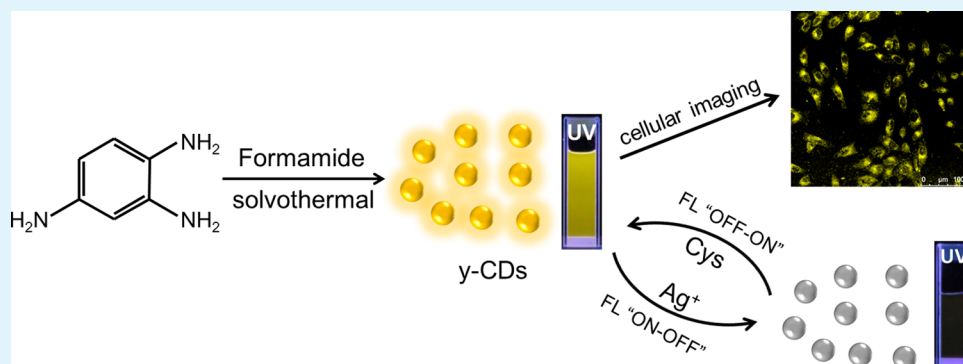
# Bright-Yellow-Emissive N-Doped Carbon Dots: Preparation, Cellular Imaging, and Bifunctional Sensing

Kai Jiang,<sup>†,‡</sup> Shan Sun,<sup>†</sup> Ling Zhang,<sup>†</sup> Yuhui Wang,<sup>\*,†</sup> Congzhong Cai,<sup>‡</sup> and Hengwei Lin<sup>\*,†</sup>

<sup>†</sup>Ningbo Institute of Materials Technology & Engineering (NIMTE), Chinese Academy of Sciences, Ningbo 315201, PR China

<sup>‡</sup>Department of Applied Physics, Chongqing University, Chongqing 401331, PR China

Supporting Information



**ABSTRACT:** Fluorescent carbon dots (CDs) have attracted much attention in recent years because of their superior optical and chemical properties, thus demonstrating many potential applications. However, the previously reported CDs mostly show strong emission only in the blue-light region, and the long-wavelength (i.e., yellow- to red-light) emissions are usually very weak. Such a drawback restricts their further applications, particularly in the biology-relevant fields. Herein, a rare example of N-doped CDs that emit bright-yellow fluorescence (i.e., y-CDs) is reported using 1,2,4-triaminobenzene as carbon precursor. The as-prepared y-CDs exhibit not only respectable emission quantum yield and highly optical stabilities but superior biocompatibility and biolabeling potentials. In addition, the y-CDs are found to show an interesting “ON–OFF–ON” three-state emission with the stepwise addition of Ag<sup>+</sup> and cysteine (Cys), indicating potential applications as a bifunctional sensing platform. Thanks to the highly intense emission of y-CDs, the gradual quenching and restoration of their fluorescence with the addition of Ag<sup>+</sup> and further Cys could also be observed with the naked eye. More importantly, the ensemble of the y-CDs and Ag<sup>+</sup> demonstrates practicability for the highly selective and sensitive detection of Cys in human plasma samples with satisfactory results.

**KEYWORDS:** carbon dots, N-doping, yellow emission, bioimaging, bifunctional sensing

## INTRODUCTION

As a new class of fluorescent nanomaterials, carbon dots (CDs) have attracted much attention in recent years.<sup>1–6</sup> Compared to the conventional semiconductor quantum dots (QDs) and organic fluorescent dyes, CDs possess numerously superior features including easy preparation and functionalization, no/low toxicity and high photostability, thus demonstrating a variety of potential applications, such as sensing, biomedicine, catalysis, and optoelectronic devices.<sup>7–13</sup> Although many kinds of CDs have been reported, most of them show intense emission only in the blue-light region, and the long-wavelength (i.e., yellow- to red-light) emissions are usually very weak. Such a drawback restricts further applications of CDs, particularly in the biology-relevant fields because of the commonly blue autofluorescence of biological matrix and photodamage of biological tissues by ultraviolet excitation light.<sup>8,10</sup> Therefore, the preparation of CDs that possess strong emission at long wavelengths is highly desirable, but this task had rarely been achieved so far.<sup>4–6</sup>

To improve and regulate fluorescence properties of CDs (e.g., quantum yields (QYs) and long wavelength emissions), surface modification and heteroatom doping are frequently employed.<sup>9–11</sup> The approach of surface modification was initially adopted to improve QYs of CDs. For instance, different types of polymers had been used to modify CDs and achieved enhancement of their QYs.<sup>2,14</sup> Because of difficulties in the removal of excess polymers, organic small molecules were applied to modify CDs later.<sup>15–19</sup> The relevant studies exhibit that types of functional groups have significant effects on fluorescence QYs of CDs but not emission maxima.<sup>16,19</sup> Recent studies showed that heteroatom doping, such as B, N, S, P, Si, and Se, could also improve emission properties of CDs.<sup>20–30</sup> Among these, N-doping was found to be very effective; thus, many kinds of N-doped CDs had been

Received: August 6, 2015

Accepted: October 1, 2015

prepared and broadly applied in sensing,<sup>24,31–33</sup> bioimaging,<sup>22,34</sup> catalysis,<sup>35</sup> and so on. To achieve N-doped CDs, two approaches (i.e., bottom-up and top-down) are generally employed. In the top-down method, biomass materials like milk and silk were taken for synthesis N-doped CDs, representing a green and economic method.<sup>22,36,37</sup> However, the as-obtained CDs usually have relatively low QYs. Thereafter, the bottom-up approach was widely used to prepare N-doped CDs by either microwave-assisted pyrolysis<sup>34,38</sup> or solvothermal treatment of nitrogen-rich molecular precursors.<sup>23,31,39</sup> Although the N-doped CDs prepared by the bottom-up approach generally hold high QYs, they usually display strong emission only in the blue-light region under ultraviolet excitation. Given that blue-light emission would be significantly interfered by the common autofluorescence of biological matrix and the potential photodamage of biological tissues by ultraviolet excitation light,<sup>8,10</sup> the previously reported N-doped CDs are hardly applied in biology-relevant fields.

Herein, the preparation of bright-yellow-emissive CDs (i.e., y-CDs) is reported using 1,2,4-triaminobenzene as carbon precursor by a facile solvothermal method, representing a rare example of N-doped CDs possessing high QYs in the long-wavelength region (i.e., intense yellow-emission). The as-prepared y-CDs exhibit excellent monodispersity, photo- and storage stability, biocompatibility, and cellular labeling capability. Moreover, the y-CDs are found to show an interesting “ON–OFF–ON” three-state emission with the stepwise addition of Ag<sup>+</sup> and cysteine (Cys), indicating potential applications as a bifunctional sensing platform. The ensemble of the y-CDs and Ag<sup>+</sup> further demonstrates practicability for the highly selective and sensitive detection of Cys in human plasma samples with satisfactory results. Finally, we want to note that red, green, and blue CDs had been achieved in our previous study,<sup>5</sup> but they do not perform very well in the fabrication of a sensing platform as do the CDs of this current system.

## EXPERIMENTAL SECTION

**Materials.** Reagent-grade of 1,2,4-triaminobenzene was purchased from Alfa Aesar (China) Chemicals Co., Ltd. Ethanol, methanol, methylene chloride, formamide, K<sub>2</sub>CO<sub>3</sub>, NaCl, Na<sub>2</sub>HPO<sub>4</sub>, MgSO<sub>4</sub>, Ca(NO<sub>3</sub>)<sub>2</sub>, glucose, and ascorbic acid (AA) were provided by Sinopharm Chemical Reagent Co., Ltd. (Shanghai, China). Arginine (Arg), serine (Ser), aspartic acid (Asp), glutamine (Glu), alanine (Ala), cysteine (Cys), homocysteine (Hcy), and glutathione (GSH) were purchased from Aladdin Chemistry Co., Ltd. (Shanghai, China). The human plasma samples were provided by Zhongnan Hospital of Wuhan University. All reagents were of analytical grade and were used as received without further purification. Deionized (DI) water was used throughout this study.

**Instrumentations.** Transmission electron microscopy (TEM) observations were carried out on a Tecnai F20 microscope. Atomic force microscope (AFM) measurements were recorded with a Veeco Dimension 3100 V. Fourier transform infrared (FT-IR) spectra were obtained on a Nicolet 6700 FT-IR spectrometer with the KBr pellet technique. Fluorescence emission and excitation spectra were measured on a Hitachi F-4600 spectrophotometer equipped with a Xe lamp under ambient conditions. UV-vis absorption spectra were recorded on a PERSEE T10CS UV-vis spectrophotometer. Fluorescence lifetime was measured with a Fluorolog 3-11 (HORIBA Jobin Yvon). XPS measurements were recorded using a ESCALAB 250Xi (Thermo Scientific). Fluorescent photographs were taken using a Canon camera (EOS 550) under excitation by a hand-held UV lamp (365 nm). The cellular imaging was carried out using confocal laser fluorescence microscopy (TCS SPSII, Leica, Germany).

**Preparation of the y-CDs.** 1,2,4-Triaminobenzene (100 mg) was first dissolved in 10 mL of formamide, and the solution was then

transferred into a Teflon autoclave. After heating at 120 °C for 12 h, the autoclave was cooled down to room temperature naturally. The reaction mixture was centrifuged at 10 000 rpm for 10 min to remove large particles. The resulting supernatant was concentrated and then purified with silica-column chromatography using mixtures of methylene chloride and methanol as eluents. After removing solvents and further drying under vacuum, the purified y-CDs are obtained as a yellow powder.

**Determination of QY.** QY of the y-CDs was determined by a widely accepted relative method.<sup>40</sup> Specially, rhodamine 6G (QY = 95% in ethanol) was selected as the reference. The QY of a sample was calculated according to the following equation:

$$\phi = \phi' \times \frac{A'}{I'} \times \frac{I}{A} \times \frac{n^2}{n'^2}$$

where  $\phi$  is the QY of the testing sample,  $I$  is the testing sample's integrated emission intensity,  $n$  is the refractive index (1.33 for water and 1.36 for ethanol), and  $A$  is the optical density. The prime symbol ('') refers to the referenced dye of known QY. To minimize reabsorption effects, absorption was always kept below 0.05 at the excitation wavelength.

**Cellular Toxicity Test.** In vitro cytotoxicity of the y-CDs was assessed by the standard MTT assay. In brief, 100 μL of MCF-7 cells were seeded in a 96-well plate with a density of  $1 \times 10^5$  cells/mL and allowed to adhere overnight. After an incubation of 24 h at 37 °C, the culture medium was discarded and cells were then treated with Dulbecco's modified Eagle's medium (DMEM) containing various concentrations of the y-CDs ( $10\text{--}50 \mu\text{g}\cdot\text{mL}^{-1}$ ) for another 24 h. At the end of incubation, the culture medium was removed, and 10 μL of MTT (5.0 mg·mL<sup>-1</sup> in PBS) was added into each well. After additional 4 h incubation, the growth medium was removed, and 100 μL of DMSO was added into each well to dissolve MTT. Finally, the optical density of each sample was recorded using a microplate reader (Imark 168–1130, Biorad, USA) at a wavelength of 550 nm.

**Cellular Imaging.** The potential of the y-CDs in biolabeling was preliminarily evaluated by their cellular imaging in the MCF-7 cells. In brief, 2.0 mL of MCF-7 cells in DMEM medium at an initial density of  $4 \times 10^4$  cells/mL were seeded in each dish and cultured at 37 °C for 24 h under a humidified atmosphere containing 5% CO<sub>2</sub>. The dispersion of the y-CDs was prepared in DMEM medium with a concentration of  $40 \mu\text{g}\cdot\text{mL}^{-1}$ . Cells were cultured with the dispersion of y-CDs for 6 h and washed three times with buffer to remove the free y-CDs. Finally, the samples were observed with confocal fluorescence microscopy.

**Detection of Ag<sup>+</sup> and Cys in Aqueous Buffer.** For the detection of Ag<sup>+</sup>, various concentrations of Ag<sup>+</sup> (0–20 μM) were separately added into the y-CDs solution ( $50 \mu\text{g}\cdot\text{mL}^{-1}$  in HEPES buffer, pH 7.2), and then subjected to fluorescence measurements after 2 min. For the detection of Cys, the y-CDs solution ( $50 \mu\text{g}\cdot\text{mL}^{-1}$  in HEPES buffer, pH 7.2) was first mixed with Ag<sup>+</sup> (10 μM); then, various concentrations of Cys were added. After 2 min, the fluorescence spectra of the mixture solutions were recorded. To evaluate selectivity of the sensor for Ag<sup>+</sup> and Cys, interferants were added instead of Ag<sup>+</sup> or Cys under the same experimental conditions. All the fluorescence spectra were recorded under excitation at 400 nm, and the emission intensity at 568 nm was recorded for quantitative analysis.

**Detection of Cys in Human Plasma Sample.** Human plasma samples were first treated using a routine procedure to remove proteins.<sup>41</sup> In brief, 0.3 mL of acetonitrile was added into a 0.1 mL human plasma sample, and the mixture was then centrifuged at 8000 rpm for 20 min. Thereafter, the supernatant was diluted 50-fold (i.e., total 200-fold dilution of the original plasma sample) and added into the solution of y-CDs and Ag<sup>+</sup> ( $50 \mu\text{g}\cdot\text{mL}^{-1}$  and 10 μM, respectively). The following operations and fluorescence measurements were the same as those for samples in the HEPES buffer. The concentrations of Cys in human plasma samples are calculated using the calibration curve obtained in aqueous buffer.

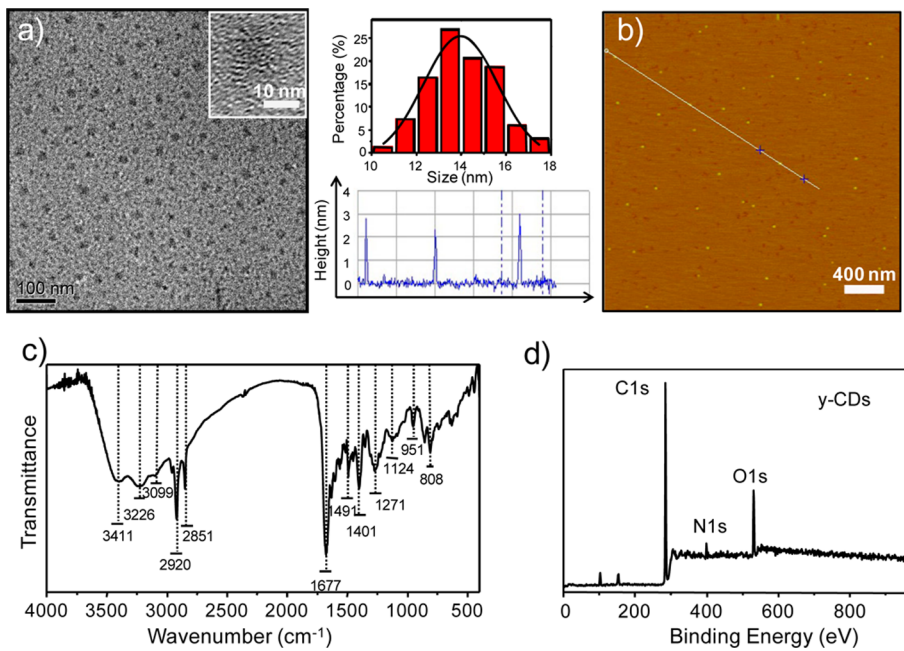


**Figure 1.** (a) TEM and (b) AFM images of the y-CDs. Middle top panel shows the TEM histogram and Gauss fitting of particle size distribution of y-CDs. Middle bottom panel shows the AFM height profile analysis along the corresponding line in (b). (c) FT-IR and (d) XPS spectra of the y-CDs.

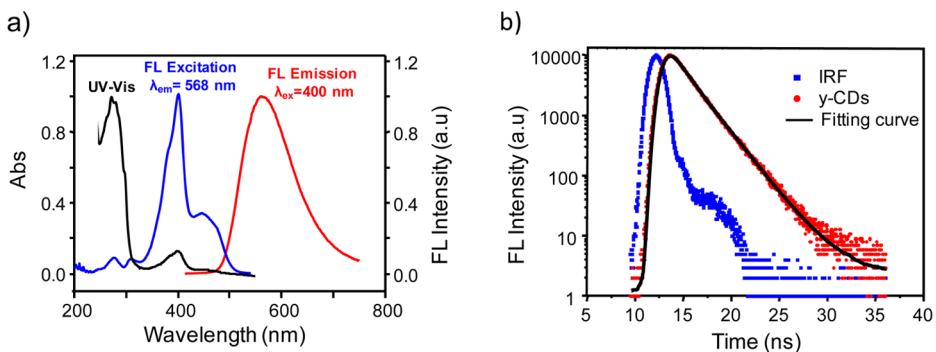


**Figure 2.** (a) Normalized UV-vis absorption (black line), FL emission (red line,  $\lambda_{\text{ex}} = 400 \text{ nm}$ ), and FL excitation (blue line,  $\lambda_{\text{em}} = 568 \text{ nm}$ ) spectra of the y-CDs in DI water. (b) FL decay spectrum and fitting curve of the y-CDs in DI water.

## RESULTS AND DISCUSSION

The yellow-emissive N-doped CDs (i.e., y-CDs) can be facilely prepared by a solvothermal method using 1,2,4-triaminobenzene as carbon precursor according to our previous report.<sup>5</sup> First, TEM and AFM characterizations were carried out to evidence our successfully obtaining CDs. As shown in Figure 1a, the y-CDs display uniform nanoparticles with average sizes about 14.3 nm, and high-resolution TEM further reveals that they are mostly noncrystalline structure because of hardly observing obvious lattice fringes (inset of Figure 1a). In addition, the AFM image shows that the y-CDs are monodispersed and exhibit similar particle heights of ca. 3 nm (Figure 1b). The observed smaller size from AFM compared to that of TEM implies that the y-CDs collapsed during the sample preparation process for AFM testing.<sup>22</sup> Then, FT-IR and XPS were carried out to characterize functionalization and chemical composition of the y-CDs. The FT-IR spectrum reveals that the y-CDs mainly contain amine (3099, 3226, and 3411  $\text{cm}^{-1}$ ), methylene (2851 and 2920  $\text{cm}^{-1}$ ), amide carbonyl (1677  $\text{cm}^{-1}$ ), C=C (1491  $\text{cm}^{-1}$ ), C–N (1401  $\text{cm}^{-1}$ ), and aromatic C–NH (1271  $\text{cm}^{-1}$ ) and C–O (1124

$\text{cm}^{-1}$ ) functional groups or chemical bonds (Figure 1c).<sup>5,22</sup> These FT-IR assignments are further verified by XPS analysis. For instance, Figure 1d indicates that the y-CDs mainly contain C, N, and O elements; the high-resolution C 1s XPS spectrum exhibits characteristic peaks of C=C/C–C, C–N, C–O, and –CONH– at 284.7, 285.3, 286.3, and 288.4 eV, respectively (Figure S1a). The high-resolution N 1s XPS spectrum exhibits the distinctive peaks of pyridine-like N, amino N, and pyrrole-like N at 398.6, 399.6, and 400.4 eV, respectively (Figure S1b); O 1s XPS spectrum shows the peaks of C–OH and C=O at 531.9 and 533.1 eV, respectively (Figure S1c).

Subsequently, the optical properties including UV-vis absorption, fluorescence (FL) emission, excitation, decay, QY, and stability of the y-CDs are fully examined. As shown in Figure 2a (black line), the y-CDs exhibit two characteristic absorption peaks at ca. 270 and 400 nm, which can be assigned to  $\pi-\pi^*$  (aromatic C=C) and n– $\pi$  (carboxyl and/or C–N) transitions, respectively.<sup>37,38</sup> Unlike most previously reported CDs, the y-CDs show an excitation-independent feature with the emission maximum at ca. 568 nm (Figure 2a, red line; i.e., a yellow emission regardless of the excitation wavelengths, Figure

S2). This observation implies that only one type of dominating emission state exists in the  $\gamma$ -CDs, which has been frequently observed as well.<sup>3,5,7–12</sup> The FL excitation spectrum of the  $\gamma$ -CDs displays a wavelength maximum at ca. 400 nm, indicating that the carboxyl and/or C–N relevant structures in the  $\gamma$ -CDs are responsible for the observed yellow emission (Figure 2a, blue line). In Figure 2b, the fluorescence decay of  $\gamma$ -CDs monitored at 568 nm represents a biexponential fitting curve with an average lifetime of 1.87 ns. Furthermore, fluorescence QY of the  $\gamma$ -CDs is determined by a widely accepted relative method.<sup>40</sup> As shown in Figures S3 and S4, the QYs of the  $\gamma$ -CDs are determined to be respectable in either organic solvent (e.g., ethanol, 32.5%, Figure S3) or DI water (10.8%, Figure S4) under excitation of 400 nm. In addition, the  $\gamma$ -CDs are observed to have relatively stable emission at broad ranges of pH (2–11), ionic strength (up to 0.5 mM NaCl), and temperature (20–40 °C) (Figures S5–S7); insignificant differences in DI water and buffer (e.g., 50 mM HEPES at pH 7.2, Figure S8); high photostability under continuous irradiation by ultraviolet light (Figure S9); and long-term storage stability under ambient conditions (Figure S10). Finally, the  $\gamma$ -CDs were also found to show solvent-polarity-dependent emission (i.e. red-shifting with enhancement of solvent polarity, Figure S11).<sup>42</sup>

Bestowed with superior optical properties (e.g., intense yellow emission and high photostability), the as-prepared  $\gamma$ -CDs are proposed to serve as a potential biolabeling reagent. To meet such an application, materials must be highly biocompatible. Hence, the cytotoxicity of the  $\gamma$ -CDs was first evaluated by the standard MTT assay. As shown in Figure 3a,

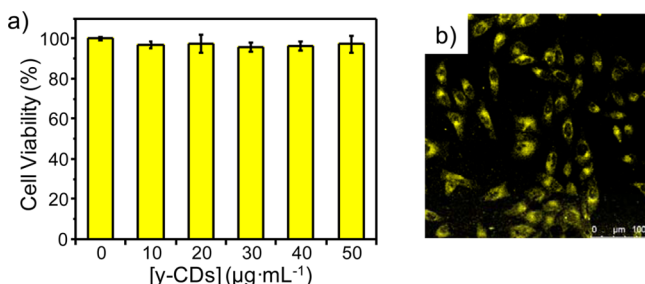


**Figure 3.** (a) Cellular cytotoxicity assessment of the  $\gamma$ -CDs using the standard MTT assay toward MCF-7 cells. (b) Confocal fluorescence image of the  $\gamma$ -CDs under 405 nm laser excitation of MCF-7 cells.

over 95% cell viability was observed after 24 h incubation of MCF-7 cells with the  $\gamma$ -CDs ( $10\text{--}50 \mu\text{g}\cdot\text{mL}^{-1}$ ). This observation confirms the very low cytotoxicity of the  $\gamma$ -CDs. To reveal potential applications for biolabeling, cellular imaging capability of the  $\gamma$ -CDs was preliminarily investigated. After

being incubated MCF-7 cells with the  $\gamma$ -CDs ( $40 \mu\text{g}\cdot\text{mL}^{-1}$ ) for 6 h, the living cells were imaged with a confocal microscope under bright-field illumination and under 405 nm laser excitation (Figure S12). The confocal image shows bright-yellow emission in MCF-7 cells (Figure 3b). It is also found from these figures that the emission mainly locates in the cytoplasm region, suggesting that the  $\gamma$ -CDs can pass through cell membranes and enter into cells.

The presence of abundant functional groups in the  $\gamma$ -CDs encouraged us to further investigate their potential sensing applications. Through broadly screening, the  $\gamma$ -CDs are found to display an interesting “ON–OFF–ON” three-state emission with the stepwise addition of  $\text{Ag}^+$  and Cys. As illustrated in a proposed sensing process (Figure 4), the observed fluorescence quenching by  $\text{Ag}^+$  could be attributed to its chelation with the  $\gamma$ -CDs, facilitating charge transfer from the excited state of the  $\gamma$ -CDs to  $\text{Ag}^+$ .<sup>43,44</sup> With further addition of Cys,  $\text{Ag}^+$  is taken away because of its stronger binding with Cys; thus, the emission of  $\gamma$ -CDs recovers.<sup>45–48</sup> These findings make the  $\gamma$ -CDs behave as a potentially bifunctional sensing platform for the recognition of  $\text{Ag}^+$  and Cys.

To obtain good sensing performances for  $\text{Ag}^+$  and Cys (e.g., limit of detection (LOD) and range of linear detection), optimizations of the usage concentrations of  $\gamma$ -CDs (e.g., 10, 25, 50, and  $100 \mu\text{g}\cdot\text{mL}^{-1}$ ) were first investigated (Figures 5, 6, and S13–S15), and the corresponding results were summarized in Table S1. Note that the concentrations of  $\text{Ag}^+$  herein were always chosen at the inflection points of its titrations to  $\gamma$ -CDs for composing the ensembles of  $\gamma$ -CDs and  $\text{Ag}^+$  for the subsequent detection of Cys. Such a selection will allow one to obtain maximum detection range and sensitivity. Through comprehensive consideration of both sensitivity (LOD) and range of linear detection,  $50 \mu\text{g}\cdot\text{mL}^{-1}$  of  $\gamma$ -CDs and the ensemble of  $50 \mu\text{g}\cdot\text{mL}^{-1}$  of  $\gamma$ -CDs and  $10 \mu\text{M}$  of  $\text{Ag}^+$  were selected as the optimized conditions for the detection of  $\text{Ag}^+$  and Cys, respectively. Then, detailed sensing performances for  $\text{Ag}^+$  and Cys using the  $\gamma$ -CDs are discussed on the basis of these optimized conditions. First, quenching kinetics observation of  $\text{Ag}^+$  to the fluorescence of  $\gamma$ -CDs demonstrates that the complexation between  $\text{Ag}^+$  and  $\gamma$ -CDs is very quick (i.e., 2 min required at most to reach equilibrium, Figure S16). Second, fluorescence titrations of the  $\gamma$ -CDs with  $\text{Ag}^+$  show a gradual quenching process with maximum efficiencies of about 90% (Figure 5a,b). Moreover, excellent linear relationships between the quenching efficiency and concentration of  $\text{Ag}^+$  from ca.  $1\text{--}7 \mu\text{M}$  are observed (Figure 5b inset), and the LOD is calculated to be  $0.20 \mu\text{M}$  according to the  $3\sigma$  (signal-to-noise) criteria.<sup>49</sup> Interestingly, the intense yellow emission of  $\gamma$ -CDs allows us to observe this gradual quenching process with increasing concentrations of  $\text{Ag}^+$  with naked eye (Figure 5c). Finally,

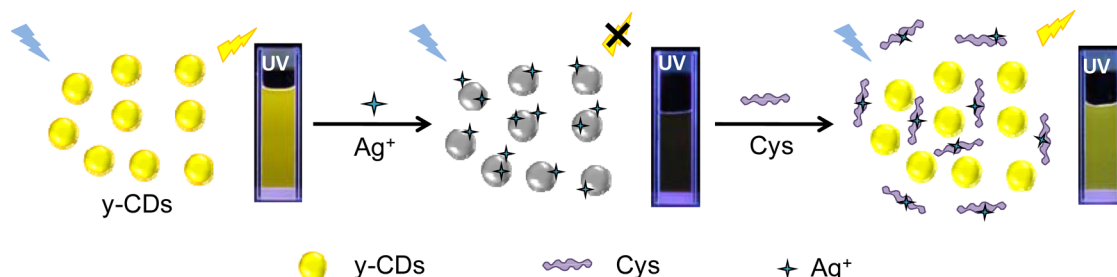


**Figure 4.** Schematic illustration of the  $\gamma$ -CDs-based bifunctional sensing platform for  $\text{Ag}^+$  and Cys.

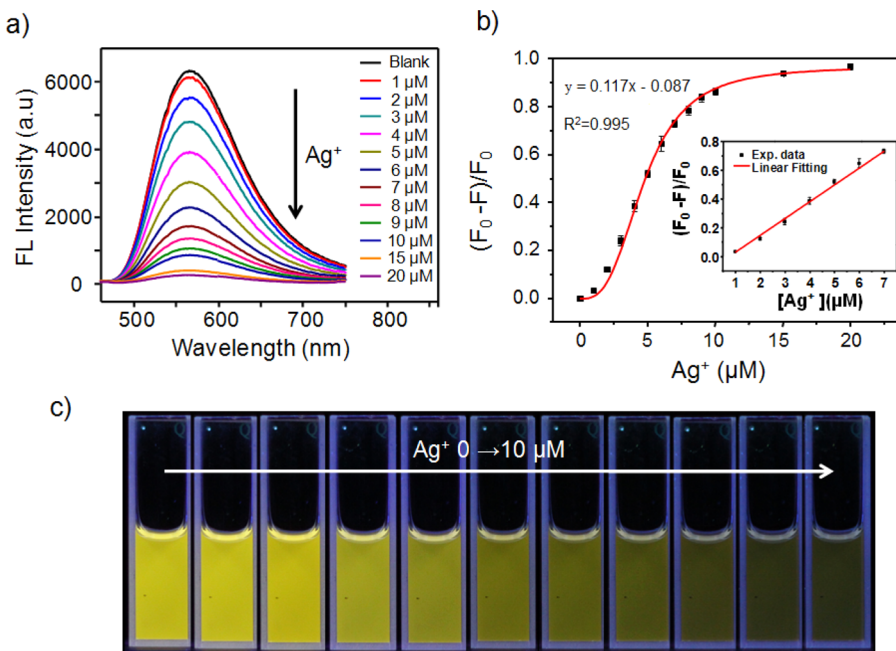


**Figure 5.** (a) Fluorescence titrations of the y-CDs ( $50 \mu\text{g}\cdot\text{mL}^{-1}$ ) with  $\text{Ag}^+$  from 1 to 20  $\mu\text{M}$ . (b) Quenching efficiency (i.e., decreases of emission intensity at 568 nm) of the y-CDs with different concentrations of  $\text{Ag}^+$ , where  $F_0$  is the fluorescence intensity of y-CDs and  $F$  is the fluorescence intensity of y-CDs with the addition of  $\text{Ag}^+$ . (c) Photographs of y-CDs with the addition of different concentrations of  $\text{Ag}^+$  under 365 nm UV lamp irradiation.

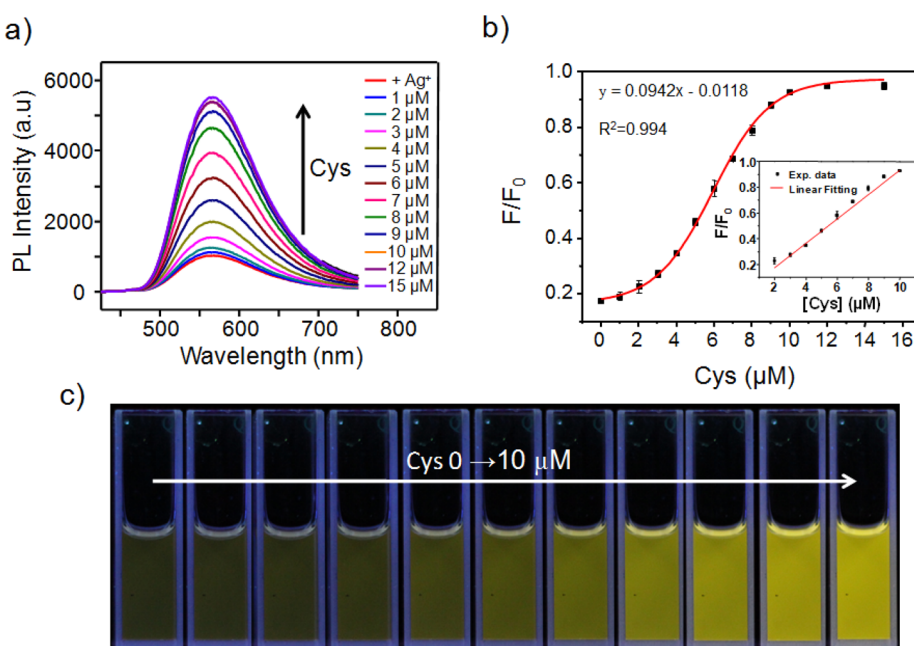


**Figure 6.** (a) Fluorescence recovery of the ensemble of y-CDs and  $\text{Ag}^+$  ( $50 \mu\text{g}\cdot\text{mL}^{-1}$  and 10  $\mu\text{M}$ , respectively) in the presence of different concentrations of Cys. (b) Relationship between fluorescence restoration of the y-CDs versus concentration of Cys, where  $F_0$  is fluorescence intensity of the free y-CDs and  $F$  is the fluorescence intensity of ensemble of y-CDs and  $\text{Ag}^+$  with the addition of Cys. (c) Corresponding photographs of the ensemble of y-CDs and  $\text{Ag}^+$  with increasing concentrations of Cys under 365 nm UV lamp irradiation.

selectivity examination of the y-CDs to  $\text{Ag}^+$  shows that none of other metal ions can cause significant fluorescence alteration, except for  $\text{Hg}^{2+}$  inducing a medium quenching (Figure S17A). The interference from  $\text{Hg}^{2+}$ , however, could be effectively eliminated by a masking agent (e.g., sulfocarbamide,<sup>50</sup> Figure S17B). These results demonstrate that the y-CDs could be potentially employed as a selective and sensitive sensor for  $\text{Ag}^+$  in aqueous media.

Given the strong thiophilicity of  $\text{Ag}^+$ , the ensemble of y-CDs and  $\text{Ag}^+$  is then proposed to design as a potential sensing platform for Cys. It is well-known that Cys is one of the most significant biothiols that play many crucial roles in human physiological processes, and abnormal levels of Cys are frequently relevant to a variety of diseases.<sup>51,52</sup> First, kinetics study reveals that fluorescence of the y-CDs could be maximally recovered (ca. 90% as of the free y-CDs) in 1 min with the

addition of Cys (Figure S18) indicating that the removal of  $\text{Ag}^+$  from the y-CDs by Cys is very fast. Second, Cys titrations of the ensemble of y-CDs and  $\text{Ag}^+$  (i.e.,  $50 \mu\text{g}\cdot\text{mL}^{-1}$  of y-CDs and  $10 \mu\text{M}$  of  $\text{Ag}^+$ ) show that the fluorescence intensity of y-CDs gradually recovers with increasing concentrations of Cys and reaches a maximum at ca.  $10 \mu\text{M}$  (Figure 6a,b). These observations demonstrate that  $\text{Ag}^+$  could be taken away effectively from the y-CDs by Cys and that complexation between them should be in a manner of 1:1 ratio. This proposed replacement process could further be evidenced by nearly no changes of fluorescence of the y-CDs with the addition of Cys (Figure S19). Importantly, a nice linear fitting is obtained between fluorescence enhancement and the concentration of Cys ranging from 2 to  $10 \mu\text{M}$  (Figure 6b inset). On the basis of this linear fitting curve, the LOD for Cys is calculated to be  $0.25 \mu\text{M}$ . This gradual enhancement of fluorescence can also be observed with naked eye with the addition of Cys from 0 to  $10 \mu\text{M}$  (Figure 6c). To evaluate the selectivity of this sensing platform for Cys, interference of common biological substances including metal ions, amino acids, and glucose, among others, are examined. As seen in Figure 7, none of these interferants cause obvious fluorescence

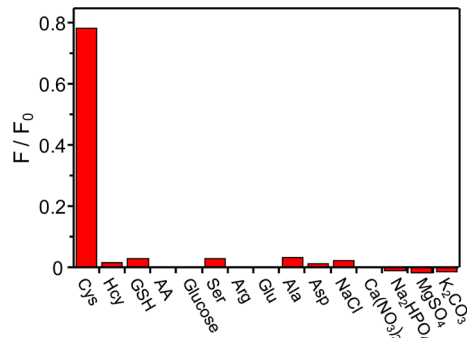


**Figure 7.** Selectivity of the ensemble of y-CDs and  $\text{Ag}^+$  ( $50 \mu\text{g}\cdot\text{mL}^{-1}$  and  $10 \mu\text{M}$ , respectively) toward Cys ( $10 \mu\text{M}$ ). Concentrations of the interferants are as follows: Hcy and GSH,  $1 \mu\text{M}$ ; ascorbic acid (AA) and glucose,  $50 \mu\text{M}$ ; Ser, Arg, Glu, Ala, Asp, NaCl,  $\text{Ca}(\text{NO}_3)_2$ ,  $\text{Na}_2\text{HPO}_4$ ,  $\text{MgSO}_4$ , and  $\text{K}_2\text{CO}_3$ ,  $1 \text{ mM}$ .  $F_0$  is fluorescence intensity of the y-CDs ( $\lambda_{\text{ex}} = 400 \text{ nm}$ ), and  $F$  is fluorescence intensity of the ensemble of y-CDs and  $\text{Ag}^+$  in the presence of Cys or interferants.

alterations. It should point out here that high concentrations of other biothiols (e.g., glutathione (GSH) and homocysteine (Hcy)) could actually induce a certain amount of fluorescence restoration of this sensing system. Nonetheless, considering that the levels of Cys in human plasma are much higher than that of GSH and Hcy (ca. 20- to 50-fold),<sup>53–55</sup> the ensemble of y-CDs and  $\text{Ag}^+$  could be implemented as a selective sensing platform for Cys in human plasma samples.

To evaluate further the practicality of the designed ensemble of y-CDs and  $\text{Ag}^+$  as a sensing platform for Cys, concentrations of Cys in human plasma samples are examined. After simple deproteination treatment of the human plasma,<sup>41</sup> 200-fold dilution samples are directly subjected to the sensing system. The concentrations of Cys in plasma samples can thus be calculated on the basis of the fluorescence enhancement using the working curve obtained above (i.e., Figure 6b). Three samples were tested, and the results are summarized in Table 1. Taking the dilution into account, Cys concentrations of the three human plasma samples are calculated to be  $320 \pm 2$ ,  $293 \pm 6$ , and  $314 \pm 6 \mu\text{M}$ , all being well-consistent with the

**Table 1. Cys Concentrations in Three Human Plasma Samples Determined Using the Proposed Method in This Study**

human plasma sample no.	spiked ( $\mu\text{M}$ )	found ( $\mu\text{M}$ )	recovery (%)	RSD (%) ( $n = 3$ )
1	0	$1.60 \pm 0.01$		0.8
	2	$3.47 \pm 0.12$	96.5	3.7
	4	$5.52 \pm 0.17$	98.6	3.1
	6	$8.34 \pm 0.20$	109.8	1.4
2	0	$1.47 \pm 0.03$		2.2
	2	$3.46 \pm 0.09$	99.9	2.5
	4	$5.43 \pm 0.08$	99.3	1.5
	6	$7.98 \pm 0.12$	106.9	1.5
3	0	$1.57 \pm 0.03$		2.1
	2	$3.61 \pm 0.32$	101.0	8.8
	4	$5.45 \pm 0.30$	97.9	5.5
	6	$7.69 \pm 0.45$	101.5	5.9

reported results by HPLC.<sup>51</sup> Moreover, standard addition experiments were carried out with these plasma samples to validate this method. As shown in Table 1, 96.5–109.8% recoveries are found with acceptable relative standard deviations (RSD) of about 5%. In addition, the observed higher values of the “found” concentrations compared to those of the “spiked” ones in this table further indicate the existence of certain amounts of Cys in the plasma samples. These results demonstrate the high robustness of the y-CDs– $\text{Ag}^+$  sensing platform for Cys in a complicated biological matrix.

## CONCLUSIONS

A rare example of N-doped CDs (i.e., y-CDs) that emit bright-yellow fluorescence is reported, which can be readily prepared via a solvothermal reaction using a common carbon precursor (i.e., 1,2,4-triaminobenzene). The as-prepared y-CDs exhibit respectable QY and high chemical and optical stabilities. Through chemical composition and structural analysis, the y-CDs are confirmed to contain various nitrogen-relevant functional groups. The cytotoxicity and cellular imaging tests demonstrate that the y-CDs possess excellent biocompatibility and biolabeling potentials. Additionally, the y-CDs are found to show an “ON–OFF–ON” three-state emission with the stepwise addition of  $\text{Ag}^+$  and Cys, indicating potential applications as a bifunctional sensing platform. Thanks to highly intense emission, quenching and restoration of fluorescence of the y-CDs with the addition of  $\text{Ag}^+$  and further Cys could also be observed with the naked eye. More importantly, the ensemble of y-CDs and  $\text{Ag}^+$  demonstrates a practical application for the highly selective and sensitive detection of Cys in human plasma samples with satisfactory results. The ongoing work in our lab is exploiting applications of the y-CDs to other kinds of crucial targets in biological systems via various functional modifications (e.g., aptamer or peptide).

## ASSOCIATED CONTENT

### S Supporting Information

The Supporting Information is available free of charge on the ACS Publications website at DOI: 10.1021/acsami.5b07255.

High resolution XPS spectra, emission properties with excitation wavelengths, QY calculation, stability and selectivity for  $\text{Ag}^+$  quenching of the y-CDs. (PDF)

## AUTHOR INFORMATION

### Corresponding Authors

\*Tel.: +86-574-86685130. Fax: +86-574-86685163. E-mail: wangyuhui@nimte.ac.cn.

\*E-mail: linhengwei@nimte.ac.cn.

### Notes

The authors declare no competing financial interest.

## ACKNOWLEDGMENTS

We acknowledge the Natural Science Foundation of China (21277149 and 21305152), Zhejiang Provincial Natural Science Foundation (LR13B050001), and Ningbo Natural Science Foundation (2014B82010 and 2015A610277). We would also like to sincerely thank Prof. Aiguo Wu and Prof. Qing Huang at NIMTE for their kind assistance in the cellular and fluorescence relevant measurements.

## REFERENCES

- (1) Xu, X.; Ray, R.; Gu, Y.; Ploehn, H. J.; Gearheart, L.; Raker, K.; Scrivens, W. A. Electrophoretic Analysis and Purification of Fluorescent Single-Walled Carbon Nanotube Fragments. *J. Am. Chem. Soc.* **2004**, *126*, 12736–12737.
- (2) Sun, Y. P.; Zhou, B.; Lin, Y.; Wang, W.; Fernando, K. A. S.; Pathak, P.; Meziani, M. J.; Harruff, B. A.; Wang, X.; Wang, H.; Luo, P. G.; Yang, H.; Kose, M. E.; Chen, B.; Veca, L. M.; Xie, S. Y. Quantum-Sized Carbon Dots for Bright and Colorful Photoluminescence. *J. Am. Chem. Soc.* **2006**, *128*, 7756–7757.
- (3) Zhu, S.; Meng, Q.; Wang, L.; Zhang, J.; Song, Y.; Jin, H.; Zhang, K.; Sun, H.; Wang, H.; Yang, B. Highly Photoluminescent Carbon Dots for Multicolor Patterning, Sensors, and Bioimaging. *Angew. Chem., Int. Ed.* **2013**, *52*, 3953–3957.
- (4) Wang, L.; Wang, Y.; Xu, T.; Liao, H.; Yao, C.; Liu, Y.; Li, Z.; Chen, Z.; Pan, D.; Sun, L.; Wu, M. Gram-Scale Synthesis of Single-Crystalline Graphene Quantum Dots with Superior Optical Properties. *Nat. Commun.* **2014**, *5*, 5357.
- (5) Jiang, K.; Sun, S.; Zhang, L.; Lu, Y.; Wu, A.; Cai, C.; Lin, H. Red, Green, and Blue Luminescence by Carbon Dots: Full-Color Emission Tuning and Multicolor Cellular Imaging. *Angew. Chem., Int. Ed.* **2015**, *54*, 5360–5363.
- (6) Hu, S.; Trinchi, A.; Atkin, P.; Cole, I. Tunable Photoluminescence Across the Entire Visible Spectrum from Carbon Dots Excited by White Light. *Angew. Chem., Int. Ed.* **2015**, *54*, 2970–2974.
- (7) Baker, S. N.; Baker, G. A. Luminescent Carbon Nanodots: Emergent Nanolights. *Angew. Chem., Int. Ed.* **2010**, *49*, 6726–6744.
- (8) Li, H.; Kang, Z.; Liu, Y.; Lee, S. T. Carbon Nanodots: Synthesis, Properties and Applications. *J. Mater. Chem.* **2012**, *22*, 24230–24253.
- (9) Wang, Y.; Hu, A. Carbon Quantum Dots: Synthesis, Properties and Applications. *J. Mater. Chem. C* **2014**, *2*, 6921–6939.
- (10) Lim, S. Y.; Shen, W.; Gao, Z. Carbon Quantum Dots and their Applications. *Chem. Soc. Rev.* **2015**, *44*, 362–381.
- (11) Zheng, X. T.; Ananthanarayanan, A.; Luo, K. Q.; Chen, P. Glowing Graphene Quantum Dots and Carbon Dots: Properties, Syntheses, and Biological Applications. *Small* **2015**, *11*, 1620–1636.
- (12) Zhu, S.; Song, Y.; Zhao, X.; Shao, J.; Zhang, J.; Yang, B. The Photoluminescence Mechanism in Carbon Dots (Graphene Quantum Dots, Carbon Nanodots, and Polymer Dots): Current State and Future Perspective. *Nano Res.* **2015**, *8*, 355–381.
- (13) Esteves da Silva, J. C. G.; Gonçalves, H. M. R. Analytical and Bioanalytical Applications of Carbon Dots. *TrAC, Trends Anal. Chem.* **2011**, *30*, 1327–1336.
- (14) Yang, L.; Jiang, W.; Qiu, L.; Jiang, X.; Zuo, D.; Wang, D.; Yang, L. One Pot Synthesis of Highly Luminescent Polyethylene Glycol Anchored Carbon Dots Functionalized with a Nuclear Localization Signal Peptide for Cell Nucleus Imaging. *Nanoscale* **2015**, *7*, 6104–6113.
- (15) Xie, Z.; Wang, F.; Liu, C. Y. Organic–Inorganic Hybrid Functional Carbon Dot Gel Glasses. *Adv. Mater.* **2012**, *24*, 1716–1721.
- (16) Zhu, S.; Zhang, J.; Tang, S.; Qiao, C.; Wang, L.; Wang, H.; Liu, X.; Li, B.; Li, Y.; Yu, W.; Wang, X.; Sun, H.; Yang, B. Surface Chemistry Routes to Modulate the Photoluminescence of Graphene Quantum Dots: From Fluorescence Mechanism to Up-Conversion Bioimaging Applications. *Adv. Funct. Mater.* **2012**, *22*, 4732–4740.
- (17) Chen, P. C.; Chen, Y.-N.; Hsu, P. C.; Shih, C.-C.; Chang, H. T. Photoluminescent Organosilane-Functionalized Carbon Dots as Temperature Probes. *Chem. Commun.* **2013**, *49*, 1639–1641.
- (18) Lai, S. K.; Luk, C. M.; Tang, L.; Teng, K. S.; Lau, S. P. Photoresponse of Polyaniline-Functionalized Graphene Quantum Dots. *Nanoscale* **2015**, *7*, 5338–5343.
- (19) Qi, B.-P.; Hu, H.; Bao, L.; Zhang, Z. L.; Tang, B.; Peng, Y.; Wang, B. S.; Pang, D. W. An Efficient Edge-Functionalization Method to Tune the Photoluminescence of Graphene Quantum Dots. *Nanoscale* **2015**, *7*, 5969–5973.
- (20) Shan, X.; Chai, L.; Ma, J.; Qian, Z.; Chen, J.; Feng, H. B-Doped Carbon Quantum Dots as a Sensitive Fluorescence Probe for Hydrogen Peroxide and Glucose Detection. *Analyst* **2014**, *139*, 2322–2325.
- (21) Bourlinos, A. B.; Trivizas, G.; Karakassides, M. A.; Baikousi, M.; Kouloumpis, A.; Gournis, D.; Bakandritsos, A.; Hola, K.; Kozak, O.; Zboril, R.; Papagiannouli, I.; Aloukos, P.; Couris, S. Green and Simple Route Toward Boron Doped Carbon Dots with Significantly Enhanced Non-Linear Optical Properties. *Carbon* **2015**, *83*, 173–179.
- (22) Li, W.; Zhang, Z.; Kong, B.; Feng, S.; Wang, J.; Wang, L.; Yang, J.; Zhang, F.; Wu, P.; Zhao, D. Simple and Green Synthesis of Nitrogen-Doped Photoluminescent Carbonaceous Nanospheres for Bioimaging. *Angew. Chem., Int. Ed.* **2013**, *52*, 8151–8155.
- (23) Zhang, Y. Q.; Ma, D. K.; Zhuang, Y.; Zhang, X.; Chen, W.; Hong, L. L.; Yan, Q. X.; Yu, K.; Huang, S. M. One-Pot Synthesis of N-Doped Carbon Dots with Tunable Luminescence Properties. *J. Mater. Chem.* **2012**, *22*, 16714–16718.
- (24) Qian, Z.; Ma, J.; Shan, X.; Feng, H.; Shao, L.; Chen, J. Highly Luminescent N-Doped Carbon Quantum Dots as an Effective Bifunctional Fluorescence Sensing Platform. *Chem. - Eur. J.* **2014**, *20*, 2254–2263.
- (25) Chandra, S.; Patra, P.; Pathan, S. H.; Roy, S.; Mitra, S.; Layek, A.; Bhar, R.; Pramanik, P.; Goswami, A. Luminescent S-Doped Carbon Dots: an Emergent Architecture for Multimodal Applications. *J. Mater. Chem. B* **2013**, *1*, 2375–2382.
- (26) Xu, Q.; Pu, P.; Zhao, J.; Dong, C.; Gao, C.; Chen, Y.; Chen, J.; Liu, Y.; Zhou, H. Preparation of Highly Photoluminescent Sulfur-Doped Carbon Dots for Fe(III) Detection. *J. Mater. Chem. A* **2015**, *3*, 542–546.
- (27) Qian, Z.; Shan, X.; Chai, L.; Ma, J.; Chen, J.; Feng, H. Si-Doped Carbon Quantum Dots: A Facile and General Preparation Strategy, Bioimaging Application, and Bifunctional Sensor. *ACS Appl. Mater. Interfaces* **2014**, *6*, 6797–6805.
- (28) Yang, S.; Sun, J.; He, P.; Deng, X.; Wang, Z.; Hu, C.; Ding, G.; Xie, X. Selenium Doped Graphene Quantum Dots as an Ultrasensitive Redox Fluorescent Switch. *Chem. Mater.* **2015**, *27*, 2004–2011.
- (29) Han, Y.; Tang, D.; Yang, Y.; Li, C.; Kong, W.; Huang, H.; Liu, Y.; Kang, Z. Non-Metal Single/Dual Doped Carbon Quantum Dots: a General Flame Synthetic Method and Electro-Catalytic Properties. *Nanoscale* **2015**, *7*, 5955–5962.
- (30) Yang, S.; Sun, J.; Li, X.; Zhou, W.; Wang, Z.; He, P.; Ding, G.; Xie, X.; Kang, Z.; Jiang, M. Large-Scale Fabrication of Heavy Doped Carbon Quantum Dots with Tunable-Photoluminescence and Sensitive Fluorescence Detection. *J. Mater. Chem. A* **2014**, *2*, 8660–8667.
- (31) Li, Z.; Yu, H.; Bian, T.; Zhao, Y.; Zhou, C.; Shang, L.; Liu, Y.; Wu, L.-Z.; Tung, C. H.; Zhang, T. Highly Luminescent Nitrogen-Doped Carbon Quantum Dots as Effective Fluorescent Probes for Mercuric and Iodide Ions. *J. Mater. Chem. C* **2015**, *3*, 1922–1928.
- (32) Gupta, A.; Chaudhary, A.; Mehra, P.; Dwivedi, C.; Khan, S.; Verma, N. C.; Nandi, C. K. Nitrogen-Doped, Thiol-Functionalized

- Carbon Dots for Ultrasensitive Hg(ii) Detection. *Chem. Commun.* **2015**, *51*, 10750–10753.
- (33) Xu, H.; Zhou, S.; Xiao, L.; Wang, H.; Li, S.; Yuan, Q. Fabrication of a Nitrogen-Doped Graphene Quantum Dot from MOF-Derived Porous Carbon and Its Application for Highly Selective Fluorescence Detection of Fe<sup>3+</sup>. *J. Mater. Chem. C* **2015**, *3*, 291–297.
- (34) Wei, W.; Xu, C.; Wu, L.; Wang, J.; Ren, J.; Qu, X. Non-Enzymatic-Browning-Reaction: A Versatile Route for Production of Nitrogen-Doped Carbon Dots with Tunable Multicolor Luminescent Display. *Sci. Rep.* **2014**, *4*, 3564 DOI: [10.1038/srep03564](https://doi.org/10.1038/srep03564).
- (35) Hu, C.; Yu, C.; Li, M.; Wang, X.; Dong, Q.; Wang, G.; Qiu, J. Nitrogen-Doped Carbon Dots Decorated on Graphene: a Novel All-Carbon Hybrid Electrocatalyst for Enhanced Oxygen Reduction Reaction. *Chem. Commun.* **2015**, *51*, 3419–3422.
- (36) Wu, Z. L.; Zhang, P.; Gao, M. X.; Liu, C. F.; Wang, W.; Leng, F.; Huang, C. Z. One-Pot Hydrothermal Synthesis of Highly Luminescent Nitrogen-Doped Amphoteric Carbon Dots for Bioimaging from Bombyx Mori Silk - Natural Proteins. *J. Mater. Chem. B* **2013**, *1*, 2868–2873.
- (37) Wang, L.; Zhou, H. S. Green Synthesis of Luminescent Nitrogen-Doped Carbon Dots from Milk and Its Imaging Application. *Anal. Chem.* **2014**, *86*, 8902–8905.
- (38) Xu, M.; He, G.; Li, Z.; He, F.; Gao, F.; Su, Y.; Zhang, L.; Yang, Z.; Zhang, Y. A Green Heterogeneous Synthesis of N-Doped Carbon Dots and their Photoluminescence Applications in Solid and Aqueous States. *Nanoscale* **2014**, *6*, 10307–10315.
- (39) Yang, Z.; Xu, M.; Liu, Y.; He, F.; Gao, F.; Su, Y.; Wei, H.; Zhang, Y. Nitrogen-Doped, Carbon-Rich, Highly Photoluminescent Carbon Dots from Ammonium Citrate. *Nanoscale* **2014**, *6*, 1890–1895.
- (40) Grabolle, M.; Spieles, M.; Lesnyak, V.; Gaponik, N.; Eychmüller, A.; Resch-Genger, U. Determination of the Fluorescence Quantum Yield of Quantum Dots: Suitable Procedures and Achievable Uncertainties. *Anal. Chem.* **2009**, *81*, 6285–6294.
- (41) Gao, X.; Li, X.; Li, L.; Zhou, J.; Ma, H. A Simple Fluorescent Off-On Probe for the Discrimination of Cysteine from Glutathione. *Chem. Commun.* **2015**, *51*, 9388–9390.
- (42) Lakowicz, J. R. *Principles of Fluorescence Spectroscopy*, 3rd ed.; Springer-Verlag: Berlin, Heidelberg, Germany, 2006.
- (43) Li, Z.; Wang, Y.; Ni, Y.; Kokot, S. A Rapid and Label-Free Dual Detection of Hg (II) and Cysteine with the Use of Fluorescence Switching of Graphene Quantum Dots. *Sens. Actuators, B* **2015**, *207*, 490–497.
- (44) Zong, J.; Yang, X.; Trinchi, A.; Hardin, S.; Cole, L.; Zhu, Y.; Li, C.; Muster, T.; Wei, G. Carbon Dots as Fluorescent Probes for "Off-On" Detection of Cu<sup>2+</sup> and L-Cysteine in Aqueous. *Biosens. Bioelectron.* **2014**, *51*, 330–335.
- (45) Tang, Y.; Song, H.; Su, Y.; Lv, Y. Turn-on Persistent Luminescence Probe Based on Graphitic Carbon Nitride for Imaging Detection of Biothiols in Biological Fluids. *Anal. Chem.* **2013**, *85*, 11876–11884.
- (46) Wang, W.; Lu, Y. C.; Huang, H.; Feng, J. J.; Chen, J. R.; Wang, A. J. Facile Synthesis of Water-soluble and Biocompatible Fluorescent Nitrogen-doped Carbon Dots for Cell Imaging. *Analyst* **2014**, *139*, 1692–1696.
- (47) Zhou, J.; Lin, Y.; Huang, Z.; Ren, J.; Qu, X. Carbon Nanodots as Fluorescence Probes for Rapid, Sensitive, and Label-free Detection of Hg<sup>2+</sup> and Biothiols in Complex Matrices. *Chem. Commun.* **2012**, *48*, 1147–1149.
- (48) Deng, J.; Lu, Q.; Hou, Y.; Liu, M.; Li, H.; Zhang, Y.; Yao, S. Nanosensor Composed of Nitrogen-Doped Carbon Dots and Gold Nanoparticles for Highly Selective Detection of Cysteine with Multiple Signals. *Anal. Chem.* **2015**, *87*, 2195–2203.
- (49) Liu, J.; Zhang, X.; Cong, Z.; Xhen, Z.; Yang, H.; Chen, G.-N. Glutathione-Functionalized Graphene Quantum Dots as Selective Fluorescent Probes for Phosphate-Containing Metabolites. *Nanoscale* **2013**, *5*, 1810.
- (50) Zaijun, L.; Qiying, Z.; Jiaomai, P. Recent Advances with Regard to Triazene Derivatives as Chromogenic Reagents in Analytical Chemistry. *Rev. Anal. Chem.* **2003**, *22*, 191–232.
- (51) Ueno, T.; Nagano, T. Fluorescent Probes for Sensing and Imaging. *Nat. Methods* **2011**, *8*, 642–645.
- (52) Seshadri, S.; Beiser, A.; Selhub, J.; Jacques, P. F.; Rosenberg, I. H.; D'Agostino, R. B.; Wilson, P. W. F.; Wolf, P. A. Plasma Homocysteine as a Risk Factor for Dementia and Alzheimer's Disease. *N. Engl. J. Med.* **2002**, *346*, 476–483.
- (53) Yoshida, Y.; Ohiwa, Y.; Shimamura, M.; Izumi, T.; Yoshida, S.; Takahashi, K.; Miyairi, S.; Makimura, M.; Naganuma, A. Optimum Conditions for Derivatization of Glutathione, Cysteine and Cysteinylglycine in Human Plasma with Ammonium 7-Fluorobenzo-2-Oxa-1,3 -Diazole-4-Sulfonate for Accurate Quantitation by High-Performance Liquid Chromatography. *J. Health Sci.* **2003**, *49*, 527–530.
- (54) Wang, Y.; Jiang, K.; Zhu, J.; Zhang, L.; Lin, H. A FREI-Based Carbon Dot-MnO<sub>2</sub> Nanosheet Architecture for Glutathione Sensing in Human Whole Blood Samples. *Chem. Commun.* **2015**, *51*, 12748–12751.
- (55) Jia, M.-Y.; Niu, L.-Y.; Zhang, Y.; Yang, Q.-Z.; Tung, C.-H.; Guan, Y.-F.; Feng, L. BODIPY-Based Fluorometric Sensor for the Simultaneous Determination of Cys, Hcy, and GSH in Human Serum. *ACS Appl. Mater. Interfaces* **2015**, *7*, 5907–5914.